The Impact of Capture on Multihop Wireless Networks in an Optimal Rate Control Framework *

Jun Jung Hyun Affan A. Syed Bhaskar Krishnamachari
University of Southern California
Los Angeles, CA 90009-0781
Email: junjn@uc.edu,asyed,bkrishna@usc.edu

ABSTRACT

We consider the end-to-end fair rate control problem in a multi-hop Aloha network with capture. Capture (also referred to as co-channel interference tolerance) occurs when a packet with a stronger signal strength can be correctly decoded at the receiver despite the presence of a weaker interfering signal. We provide an approximate model for the link capacity with capture and incorporate it into a cross-layer joint link/session rate optimization framework. We show that this is a convex optimization problem and then present a sub-gradient algorithm for realistic distributed implementation in a network. Through analysis and simulations, we quantify the improvement in performance obtained with capture. We find that the capture effect benefits primarily low-contention links and non-bottle-neck sessions. As a result, although capture provides significant improvements in the total throughput (sum rate), it seems to provide little improvement in the objective function (sum of the logarithm of the rates).

Categories and Subject Descriptors

C.2.4 [**Computer-Communication Networks**]: Distributed systems

General Terms

Algorithms

Keywords

Cross-layer control, ad-hoc network, random access

1. INTRODUCTION

*The work described here is supported in part by NSF through grants CNS-0347621, CNS-0627028, CCF-0430061, CNS-0325875, and by the National Aeronautics and Space Administration through an AIST grant

WICON 2007, October 22-24, Austin, USA

DOI 10.4108/wicon.2007.2095

In much of the literature on the design and analysis of higher-layer protocols in multi-hop wireless networks, a simple model has been used to analyze link quality in the presence of multiple concurrent transmitters. In this simple *protocol model*, when two nodes within a given range of a given receiver transmit simultaneously, their transmissions result in a collision. A more realistic model is the *capture model*, wherein a transmission can be successfully received even in the presence of other nearby transmissions so long as the signal-to-interference-ratio (SINR) exceeds a given threshold. Although in theory the protocol model may offer a simple but effective approximation, recent empirical studies [4, 5] show a significant degree of capture effect. In light of these findings, it is important to examine how cross-layer protocols can be designed taking the capture effect into account, and how this impacts the overall network performance.

We study the impact of capture in the framework of a cross-layer optimization problem first formulated by Wang and Kar [2]. This work considers the joint optimization of the link and transport layers. At the link layer, a slotted Aloha protocol is used for medium access and the tunable parameter is the access probability for each link. At the transport layer, the tunable parameter is the value of the session rate for each end-to-end flow. The authors of that work formulate this as a network utility maximization problem and provide primal and dual-based algorithms for it. The objective function is fairness-oriented and maximizes the sum of the log of the session rates.

The following are our contributions in this work:

- We enhance the joint link-transport optimization problem by explicitly building in a model based on outage probability to approximate the capture effect and study how this impacts link capacities and the overall session rates.
- We show that the enhanced problem can also be expressed as a convex optimization problem and extend for this case a distributed sub-gradient algorithm for efficient network implementation.
- We systematically investigate the performance of the algorithm through analysis and simulations in the context of simple topologies (circular, exponential-distance and linear-distance) as well as large-scale generated topologies.
- We find that taking into account the capture effect can provide significant improvement in the total throughput (sum of the session rates). However, at the same

time, there are only negligible improvements in the sum-log utility function. This appears to be the result of a rich-get-richer/poor-remain-poor behavior when capture is considered. The capture effect seems to benefit primarily the good quality links and non-bottleneck sessions using those links.

There is a delicate balance to be achieved in any modeling effort between realism and tractability. If one were to build a capture model considering all possible concurrent transmission scenarios, it would require the number of terms for each link to grow exponentially with the number of neighbors of the receiver.

While we do provide an exact solution for a simple circular topology, for tractability we have chosen to consider capture only in the case of pairwise contention, i.e., when there are two concurrent transmissions. One justification for this approximation is that the probability of successful transmission is lower when there is more than one interfering node (as the SINR becomes smaller). It remains to be seen how tight this approximation is in the case of highly loaded dense networks, but in any case, it provides a lower bound on the improvement that can be obtained by considering the capture effect.

Related Work: Recently, the topic of cross-layer optimization in multi-hop wireless networks has received growing attention. With respect to the modeling of the link layer capacities, some of the prior work has focused on CDMA scenarios in which a rate is a logarithmic function of the SINR [6, 7]. Others have advocated the use of graph-cliques to model contention [8]. To our knowledge, the work by Wang and Kar [2] is the first to look at the joint link-transport layer optimization in the context of contention using slotted Aloha random access, but they use the simple protocol model in which any concurrent transmission event is treated as a packet loss. A significant motivation for our work is that although much of the design and analysis of higher layer protocols in multi-hop wireless networks has ignored this capture effect, recent empirical studies suggest that the capture effect is a significant factor in practice [4, 5].

2. PROBLEM FORMULATION

We consider end-to-end proportionally fair rate control problem in a multi-hop Aloha network with capture as described below. This problem formulation is parallel to the one by Wang and Kar [2]. *Capture effect* (or *co-channel interference tolerance*), is when a stronger signal *captures* the channel such that in spite of an existing weaker signal, it can be correctly decoded at a receiver. Our objective is to maximize the proportional fairness of the shared bandwidth in the wireless network, while specifically taking the capture effect into account.

We model the wireless network as a network graph G=(V,E), where V is the set of nodes and E is set of undirected edges connecting nodes within a specified distance. A directed link (i,j) will represent an active communication path between, and we name L as the set of such active paths. The distance between node i,j is defined as the euclidean distance $d_{i,j}$. We specify, for each node i its neighborhood N^i. Additionally O^i and I^i and are the set of outgoing and incoming neighbor of node i (defined on the basis of an active incoming or outgoing link). The transport layer sessions are represented by the set S. Let $L(s) \subseteq L$ denotes the set of active links a session $s \in S$ uses. Also S(i,j) represents the set of sessions on a link (i,j) that belongs to S.

2.1 Link Rates: with and without capture

Assuming slotted Aloha for the link access [9], each node has a probability P_i of transmitting in a given slot. Each node has $p_{i,j}$ as the accesses probability, that it can control, to transmit on a particular outgoing link. $\vec{p} = (p_{i,j}.(i,j) \in L)$, be the vector of transmission probabilities on all edges. Then we can define the rate on any link (i,j), in slotted Aloha, as the following expression:

$$x_{i,j} = c_{ij}(\vec{p}) = p_{i,j}(1 - P_j)(f(i,j) + g(i,j)) \qquad (1)$$

Here, for both without and with capture cases

$$f(i,j) = \prod_{k \in N^j/\{i\}} 1 - P_k$$

representing the case where no neighbor of the receiver attempts any contention at all. In all works, to our knowledge, the second term $g(i,j)$ has been considered as follows:

$$g(i,j) = 0;$$

This is the classical "collision as failure" protocol model prevalent in the existing literature.

Capture Model:

We now consider the case when capture can occur. For mathematical tractability, we do not consider all possible cases resulting in capture. Instead we look at all cases where one of the neighbor, (k) of sink j, interferes with the transmission from i to j. This gives us the following expression:

$$g(i,j) = \sum_{k \in N^j/\{i\}} P_k \alpha_{i,j,k} \Big(\prod_{l \in N^j/\{i,k\}} (1 - P_l) \Big)$$

where,

$$\begin{aligned} \alpha_{s,t,k} &= \frac{TP_{s,t}/d^2_{s,t}}{TP_{s,t}/d^2_{s,t} + (SINR_{th})TP_{k,t}/d^2_{k,t}} \\ &= \frac{1}{1 + (SINR_{th})\frac{TP_{kt}/d^2_{kt}}{TP_{st}/d^2_{st}}} \end{aligned} \qquad (2)$$

This term represents the probability of the event that a node k, in the neighborhood of j, will interfere with node i's transmission, and i will win due to capture.

The $\alpha_{s,t,k}$ term represents the success probability for the transmission from s to t, with k as interferer derived from the standard equation for the outage probability when only two nodes interfere. Details are provided in the appendix.

Note that this $g(i,j)$ term underestimates the increase in capacity obtained by capture (which would have to consider all combinations of the $|N^j - 1|$ transmitting and i still succeeding). To consider all combinations, in a general topology, requires exponentially long expressions in the optimization formulation. Although our model ignores higher combinations for reasons of tractability, this need not be a significant deviation from the actual benefit to be gained by capture for reasons explained earlier. In any case, our results give us a lower bound on the benefit that capture can provide.

2.2 Problem Statement

So now we formulate the cross layer optimization where we assume logarithmic utility function for the session in our networks. This allows us to keep close to the work in [2], which we will use for comparison.

Original Problem:

$$max \sum_{s \in S} \log y_s \tag{3}$$

subject to

$$\sum_{s \in S(i,j)} y_s \leq x_{i,j}$$

Rate constraints:

$$x_{i,j} = c_{ij}(p) \quad \forall i, j \in L$$

Probability constraints:

$$\sum_{j \in O^i} p_{i,j} = P_i \quad \forall i \in V$$

$$0 \leq P_i \leq 1 \quad \forall i \in V$$

$$0 \leq p(i,j) \leq 1 \quad \forall i, j \in L$$

$$0 \leq y_s \quad \forall s \in S$$

This formulation is essentially the same as in [2]; the change being the expression for link rate in the rate constraint. This also indicates that, at least intuitively, considering capture only increases the rate available at the link layer, and thus the transport layer mechanisms for optimization should not change. This will in fact be borne out in the convex solution to this problem described in the next section.

The current problem in (3) is not convex, due to the rate constraint. In the next section we transform it to a convex problem, to propose a centralized solution.

3. CONVEX FORMULATION AND CENTRALIZED ALGORITHM

To solve the problem in (3), we follow the same technique as in [2]. Notice this transformation does not lose the generality of the problem itself, and is very similar to the geometric programming technique.

Let $z^s = \log(y_s)$ we transform the rate constraint into a convex problem by taking logarithm of the rate constraint. The transformed equation is convex and can be solved using a non-linear optimization solver such as LOQO [3], in a centralized manner.

The equivalent problem to (3) can now be formulated as:

Convex Problem:

$$max \sum_{s \in S} z^s \tag{4}$$

$$\text{s.t. } \forall (i,j) \in L$$

$$\log\Big(\sum_{s \in S(i,j)} e^{z^s}\Big) - \sum_{k \in N^j \setminus i} \log(1 - P_k)$$

$$- \log p_{ij} - \log(1 - P_j) - \log\Big(1 + \sum_{k \in N^j \setminus i} \beta_{s,t,k}\Big) \leq 0,$$

$$0 \leq p(i,j) \leq 1$$

$$\beta_{s,t,k} + \frac{P_k \alpha_{s,t,k}}{1 - P_k} \leq 0, \ \forall s, t, k \in V$$

$$\frac{P_k \alpha_{s,t,k}}{1 - P_k} - \beta_{s,t,k} \leq 0, \ \forall s, t, k \in V$$

$$\sum_{j \in O^i} p_{i,j} = P_i \quad \forall i, j \in V$$

$$0 \leq P_i \leq 1 \quad \forall i \in V$$

This problem (4) is convex since (a) constraints 3 and 4 are convex (see appendix for the proof of this claim) (b) the first (capacity) constraint is convex since the last term , $\log(1 + \sum_{k \in N^j \setminus i} \beta_{s,t,k})$, is concave; and (c) the convexity of the remaining terms in this constraint is proved in [2].

3.1 Distributed Algorithm

Our prime motivation is to demonstrate the importance of considering capture. We extend the modified version of the distributed algorithm present in [2]. We relax the capacity constraint in (4), and then solve the resulting problem with a sub-gradient algorithm, which we then use for running on large scale random topologies. This verifies the practicality of the algorithm (as it is distributed), but also allows us to look at the trends when comparing the problem with and without considering capture.

Let $z = (z_s, s \in S)$, and $w = (p, z)$. We then define $U_s(w) = z_s$ for end user $s \in S$, and

$$g_l(w) = \log\Big(\sum_{s \in S(i,j)} e^{z^s}\Big) - \log p_{ij} - \log(1 - P_j) - \sum_{k \in N^j \setminus i} \log(1 - P_k) - \log\Big(1 + \sum_{k \in N^j \setminus i} \frac{P_k \alpha_{st,k}}{1 - P_k}\Big) \ \forall l \in L$$

Now we consider following optimization problem.

Distributed Problem:

$$max \sum_{w \in W} U_s(w) - \kappa \sum_{l \in L} \max\{0, g_l(w)\} \tag{5}$$

$$\text{s.t.}$$

$$w \in W$$

Here W represents the region in which $0 \leq p_{ij} \leq 1$ for any link $(i,j) \in L$ and P_i for any nodes $i \in N^j$ which satisfies $\sum_{\forall i} P_i = 1$. In the distributed algorithm we do a projection onto this region for conformance to the requirements. κ is a "penalty factor", which is a large positive constant (1000 in our case).

We now present the sub-gradient method to solve it in an distributed, iterative manner.

For each link $(i,j) \in L$, define the link congestion indicator for link (i,j) at the nth iteration, $\varepsilon^{(n)}_{(i,j)}$,as

$$\varepsilon^{(n)}_{(i,j)} = \begin{cases} 0 & if \sum_{s \in S(i,j)} e^{z_s^{(n)}} \leq x^{(n)}_{(i,j)} \\ 1 & otherwise \end{cases} \tag{6}$$

We use the gradient descent method to solve this optimization problem by updating the z_s and link attempt probabilities using the following equations (7) and (8) . The γ_n is step size which is a small positive constant which we currently tune to ensure convergence under different densities.

$$z_s^{(n+1)} = z_s^{(n)} + \gamma_n \left(1 - \kappa \sum_{s \in S(i,j)} \frac{\varepsilon^{(n)}_{(i,j)} e^{z_s^{(n)}}}{\sum\limits_{r \in S(i,j)} e^{z_r^{(n)}}} \right) \tag{7}$$

$$p^{(n+1)}_{(i,j)} = p^{(n)}_{(i,j)} - \gamma_n \kappa \sum_{(s,t) \in L} \frac{\varepsilon^{(n)}_{(i,j)}}{x^{(n)}_{(s,t)}} \frac{\partial c_{st}}{\partial p_{(i,j)}} (p^{(n)}), \tag{8}$$

Note the capture event does not affect the update for the rate of session s directly. Where as, it has a direct affect on the updates of attempt probability on link (i,j). $\frac{\partial c_{st}}{\partial p_{(i,j)}}(p)$ depicts how the attempt probability on link (i,j) impacts the rate on link (s,t); note that this impact is weighted by the inverse of the rate on that link as shown below.

$$\frac{\frac{\partial c_{st}}{\partial p_{(i,j)}}(p)}{x_{ij}} = \begin{cases} \frac{1}{p_{st}} & \text{,if } t = j \text{ and } s = i \\ \frac{-1}{1-P_t} & \text{,if } t = i \text{ and } s \in I_t \\ \frac{-1}{1-P_i} \left(1 - \frac{\alpha_{st,i} + \frac{P_i \alpha_{st,i}}{1-P_i}}{1 + \sum\limits_{k \in N^t \setminus \{s\}} \frac{P_k \alpha_{st,k}}{1-P_k}} \right) & \\ \text{,if } t \in N^i \text{ and } s \in I_t \setminus \{i\} & \\ 0 & \text{, otherwise} \end{cases} \tag{9}$$

Also note that it is the third case, $t \in N^i$ and $s \in I_t \setminus \{i\}$, where capture affects the rate on link (i,j). This can be verified by comparing to similar update equations, but without capture in [2].

The resulting distributed algo is described in the following pseudo code:

Algorithm 3.1: DISTRIBRATECONTROL(p_{init}, y_{init}, Υ)

Initialize :
$\forall i \in V$
$\begin{cases} \forall j \in O^i \\ n \leftarrow 0 p^n_{i,j} \leftarrow p_{init} \\ z^n_s \leftarrow log y_{init} \forall S(i,j) \end{cases}$
Iterate :
while $((P^n_i - P^{n-1}_i) > \Upsilon)$
do $\begin{cases} \forall i \in V \forall j \in O^i \\ \epsilon^n_{i,j} \leftarrow \text{as in (6)} \\ p^n_{i,j} \leftarrow \text{as in (8)} \\ z^n_s \leftarrow \text{as in (7)} \ \forall S(i,j) \\ n \leftarrow n+1 \end{cases}$

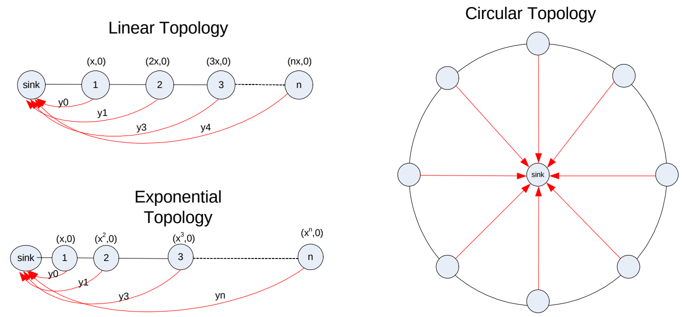

Figure 1: The set of topologies used in our micro-analysis

4. EXPERIMENTS FOR MICRO-ANALYSIS

4.1 Convergence of Sub-Gradient Algorithm

In order to confirm that our sub-gradient algorithm is accurate, we compare its result for three simple topologies (Figure 1), with those obtained from LOQO [3]. In each topology, there is only one sink, and all session occur over a single link. The positioning of nodes relative to the sink gives that topology name i.e. equidistant is circular topology, linearly and exponentially increasing distance to the sink gives the other two topologies. These three sample network topologies were chosen for their simplicity in understanding behavior and ease of modeling in LOQO.

Table 1 shows the optimal utility $(\sum Log(y_s))$ for these topologies (for only 4 nodes) as obtained by the simulation and through LOQO. There is a very small difference in the optimal value, within tolerable limits. This difference can be made arbitrarily smaller by either choosing smaller step size or making the choice of step size dynamic [10]. However, this optimization of the algorithm is not the focus of our research.

Another interesting observation is that with linear and exponential topologies have better network utility than the circular topology.

4.2 The impact of capture: neighborhood density

In order to compare what benefit capture provides us, we decided to use the circular topology where we varied the neighborhood of the sink. In many sense this topology is the most fairest to use for comparison. One reason is that with a circular topology, all nodes are equal – just as they are in the without capture scenario, where node distances are not considered. Thus for the without capture case, we have just a single topology with n nodes in its neighborhood, for comparison with all three (circular, linear, and exponential) topologies. Another reason is that (as is apparent from Table 1) the equidistant topology is the "worst case improve-

Topology	*Circular*	*Linear*	*Exponential*
Sub-Gradient Algorithm	-8.015972	-7.677260	-7.413396
Global Optimum(LOQO)	-8.01481	-7.66038	-7.34843

Table 1: Verifying convergence of the sub-gradient algorithm by looking at the optimal utility of different topologies

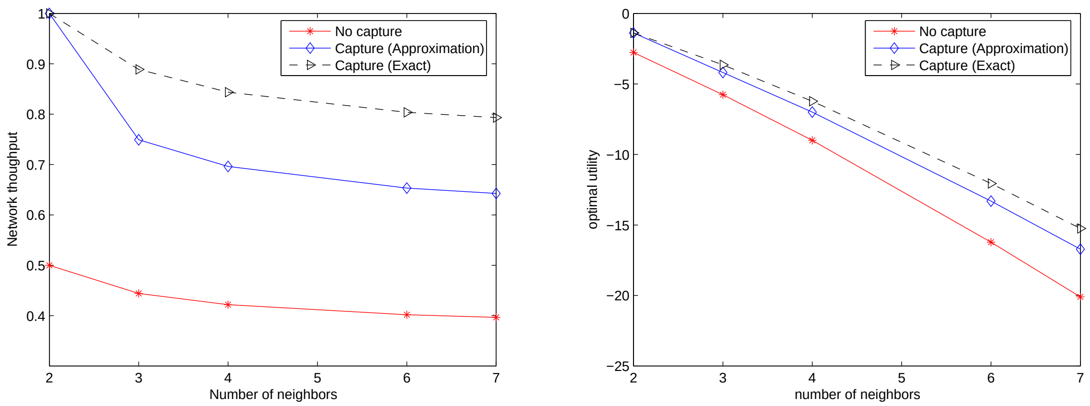

Figure 2: At $SINR_{th}$= 1 Network throughput and Network utility for circular topology

ment" that we can obtain by considering capture.

Interestingly, for this simple circular scenario, there is an easy characterization of the original optimization problem in (3). The simplification stems from the fact that with the one session per link, and a single sink, proportional fairness results in all nodes being assigned the same access probabilities (also note that there is only one outgoing link for each node, so $P_i = p_{i,sink} = p$).

Furthermore, each node assigns its session to be equal to the link capacity obtained at the particular optimal access probability. This is because each node can do only worse (as utility is monotonic increasing) by not making its session rate equal to the link capacity. This results in converting the first inequality constraint in (3) to an equality. This transformation is valid as we know there is only one link over which the session exists.

Now with these reductions the optimization problem becomes:

With Capture - approximate:

$$maximize \left(n \log(p(1-p)^{n-1} + \alpha_{st,k}(n-1)p^2(1-p)^{n-2}\right)$$

subject to

$$0 \leq p \leq 1$$

Without Capture:

$$maximize \left(n \log(p(1-p)^{n-1}\right)$$

subject to

$$0 \leq p \leq 1$$

By solving this using simple optimization techniques, we obtain that for the without capture case the optimal $p* = 1/n$, where n is the neighborhood size. A similar solution for the *with* capture case, however resulted in a quadratic solution, with only one root satisfying the probability constraints.

For the purposes of quantifying our deviation from the exact model where all possible events where we consider capture, we also provide an exact formulation for the circular topology. Here we look at all possible combination of interferers and based on the outage probability model in [1], formulate the problem as follows:

With Capture - Exact:

$$maximize \left(n \log\left(\sum_{k=1}^{n} (\frac{1}{2})^k \binom{n-1}{k} p^{k+1}(1-p)^{n-1-k}\right)\right)$$

subject to

$$0 \leq p \leq 1$$

Here the probability of different combinations of interferers happening are weighed by $(\frac{1}{2})^k$, which is the probability of that the k interfering event will result in capture, where $\frac{1}{2}$ represents the success probability for a single pair of interferers at $SINR_{th}$=1.

The result of these analysis are shown in Figure 2. We refer to the sum of the session rates as the network throughput. We also use the solution from the exact capture formulation above as an upper bound in this simple scenario.

The first observation is that as density increases the overall benefit decreases for both the capture and without capture case. To bound the underestimation due to our approximate modeling, Figure 2 also shows that there is some decrease (16-18%) from the exact formulation, for both throughput and utility, where all capture possibilities are considered vs when we use our approximate model. This decrease seems to be fairly constant for all densities, and provides us the absolute bound by which our model will deviate from the actual gains that capture can provide. However, note that this difference is for a specific topology (equidistant) with assumptions about the radio ($SINR_{th} = 1$). For a more realistic, high density/load network it remains to be seen how tight this approximation might be; however the intuition is that there will be a similar deviation from the best case capacity gains that can be used by considering capture.

Also, as Figure 3 shows, the percentage improvement in throughput at different densities (for our approximate mode vs the without capture model) is fairly constant at 65% ($SINR_{th}$=1). Even for bad radios, with $SINR_{th} > 3$, we observe the trend to be similar and a fairly healthy gain of 25% is observed.

Looking at the utility curve in Figure 2 seems to show a similar trend; even the exact case results in a decrease in utility as density increases. As a result, even the percentage decrease in utility from the exact case in our approximation is much less than for throughput.

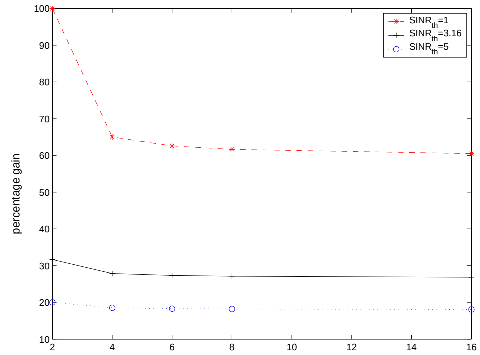

Figure 3: Percentage utility gain and network throughput gain by considering capture at different $SINR_{th}$.

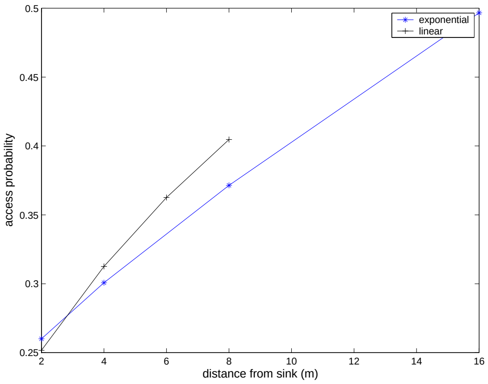

Figure 4: Access probability for linear and exponential topology

The reason seems to be that at higher density, each individual session (which in our case is also the link capacity) has to be assigned a lower value, and this results in a overall decrease in the network utility.

4.3 The impact of capture in rate control: optimal access probability

Another interesting micro-experiment involves looking at how the access probabilities assigned to different topologies (Figure 4). In the circular case, as expected, all nodes get the same probability assigned, regardless of their distance from the sink. This probability is dependent on the number of nodes, or the neighborhood density. However, for the exponential (and very similarly for the linear case), the assignment is such that nodes closer to the sink (with the highest benefit to gain from capture) actually gets assigned the lowest access probability and thus gets s lower capacity. The furthest node however gets assigned probability that increases in a linear fashion with the distance. This is due to the proportional fairness objective of the algorithm, as the further node needs to attempt at a higher probability to gain benefits comparable to the closer node.

5. LARGE SCALE MULTI-HOP SIMULATIONS FOR MACRO-ANALYSIS

5.1 Simulation setup

In order to observe the effect of capture on a macro scale, we decided to run large scale simulations. For our simulations, we randomly deployed nodes on a 8x8 grid, with each unit equal to 50m. We considered a nominal transmission range of 100m (typical of current sensor net radios) We make sure that the topology is a connected by running a DFS before generating sessions by executing a pseudo random walk (pseudo random as we ensure that our next hop is geographically away from the last hop). If we encounter a dead end, we stop, otherwise we choose a route for a maximum of five hops.

Since a particular topology is only pertinent if all nodes are either source or router for some session, we keep on generating sessions in the above manner until all nodes are participating in some manner.

To observe the effect of node density, we change a parameter, *density scale*, that is basically the percentage of the 64 node positions that are filled in our grid (e.g. density scale of 0.5 implies a random topology with 32 nodes). We run the simulations up to a density scale of 0.8 since higher densities took a very long time for convergence. As table 2 shows, the neighborhood size and session count increases as we increase the scale and thus allows us to comment on the behavior under different neighborhood densities. For purposes of averaging out outliers, we average the simulation results at each density scale over 100 simulation runs. All our graphs show error bars giving 95% confidence intervals.

5.2 Effect of density for multi-hop networks

As a first investigative step we look at three different metrics (network throughput, throughput gain, and network utility) for two different types of radios ($SINR_{th} = 1 \textit{ and } 3.16$). A good radio is represented by the extreme case of $SINR_{th} = 1$ as then a signal even slightly above the noise floor will be received. The $SINR_{th} = 3.16$, represents a typical radio used in low cost wireless platforms such as the mica motes. The two radios are chosen based on their representative nature used in wireless network research and also to give a feel of when capture effect is the most significant.

The results of the simulations are summarized in the Figures 5 and 6. The throughput of the network seems to reach a peak (in both the good and typical radio case) at around a density scale of 0.4, with a considerably higher peak when we consider capture. The percentage gain in the throughput with capture, seems to remain constant over nearly all density scales. What is most interesting is that the constant percentage gain in throughput matches very closely the values obtained for the simple circular topology (Figure 3) for the corresponding threshold values, i.e., approximately 40% gain at $SINR_{th}$ =3.16 and 70% at 1. On the other hand, although there are definite improvements in the network utility, it obviously does not increase by the same amount. This requires further investigation that is provided

density scale	*0.2*	*0.4*	*0.6*	*0.8*
average neighbors	1.7667	3.1333	5.2333	7.1000
average sessions	4.6000	11.0333	15.6333	20.6667

Table 2: Average neighborhood size generated at different density scales

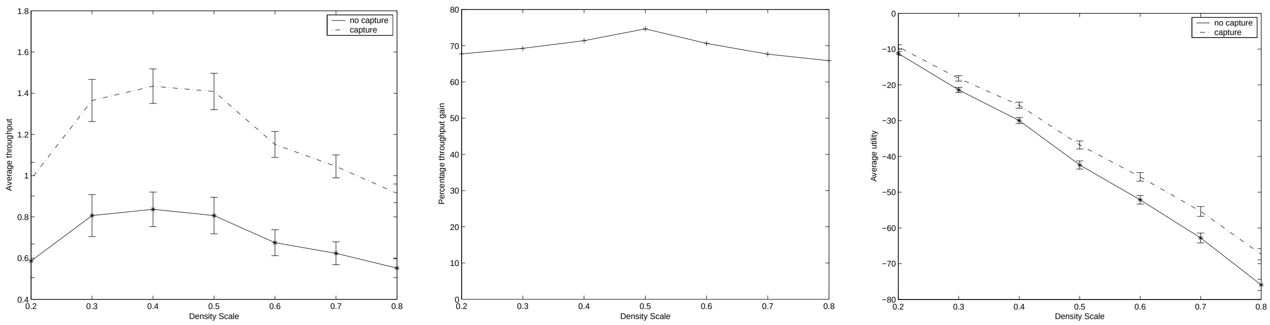

(a) (b) (c)

Figure 5: At $SINR_{th}$= 1,(a) Network throughput (b) Percentage throughput gain (c) Network utility at different density scales

in the next section.

5.3 Change in session rates and link capacities

After observing that the network utility does not give as much benefit as the network throughput does, we decided to look at how capture changes the values of individual sessions rates and how does the capacity of each link varies.

For this we considered three sets of topologies. Small (density scale=0.3), Medium (density scale=0.5), and Large (density scale=0.8). These results were performed for two different $SINR_{th}$ of 3.16(typical radio, Figure 8) and 1(good radio,Figure 7). These figures plot a pareto histogram of the session rates, ordered in respect to their session rate in the without capture scenario.

From Figure 8 we can see the "rich-get-richer/poor-stay-poor" behavior. What seems to happen is that the sessions that already had a high rate in the without capture formulation, were exactly the ones that get the highest gains in terms of throughput. The highest session, at all densities, invariable gets a more than 100% increase in its rate. At the same time, the sessions with the small rates do not seem benefit when capture is consider in the optimization formulation. This trend is replicated no matter what type of radio is considered. However, with a better radio (smaller $SINR_{th}$), there are many more sessions that get an improvement in their rates.

Since the sessions with low initial (before considering capture) rates are the one that must have a bottle-neck link, we need to examine in detail how the capacities of individual links change.

Figure 10 and 9 show the change in link capacities of the nodes (arranged in decreasing order of their initial link capacities). It is quite apparent that the more bottle-necked nodes do not get any capacity increase in the proportionally fair optimization frame work even when capture effect is taken into account. Instead, the nodes which already have a high capacity are the ones who benefit from considering capture in the optimization framework. For the lower $SINR_{th}$, the tail of the graph seems to be much more heavier than for the higher value, and thus the capacity seems to increase more uniformly over all initial link capacities. Interestingly the capacity of a few links actually decreases in this formulation.

These result do explain why the utility of the network does not increase in proportion to the overall throughput increase. This is because the sessions with initially high session rates (already in the flat portion of the utility curve) are the ones that get their rates increased the most - with very little improvement in utility. On the other hand, the starved sessions, where even a small rate increase gives high utility gains, are the ones whose rate increases negligibly or not at all. This is the rich-get-richer/poor-stay-poor effect.

There is a caveat to these observations; the fact that the bottle-neck links do not get any substantial benefit might be affected by our model that underestimates the capture gain. However, the intuition is that the overall trend should remain the same. This is supported by comparing the session rate and capacities for the two different $SINR_{th}$. In some sense we compensate for the difference in our capture modeling at $SINR_{th} = 3.16$ by looking at the results for a $SINR_{th} = 1$, where capture gives higher benefit.

6. CONCLUSION

We have shown how the joint link-transport layer optimization problem and its distributed solutions can be enhanced to incorporate the capture effect by an approximate model.

Our analysis of the small and large scale experiments shows consistently that capture effect significantly improves the total throughput but the increase in the sum-log utility function is not as high. This is due to a "rich-get-richer/poor-stay-poor" effect for both session rates and link capacities.

Future work will include investigation of how accurate our model is in estimating the impact of capture effect (for instance, by comparing it with brute-force solutions considering all possible concurrent transmissions). Another promising area is joint link-routing-transport layer optimization as it appears that with increased capacity being provided by capture, it would be even more beneficial to change bottlenecked session routes to go over links with higher capacity.

7. ACKNOWLEDGMENTS

We would like to thank Wang Xi, Dongjin Son, Apoorva Jindal, and Fernando Ordonez for their assistance and advice.

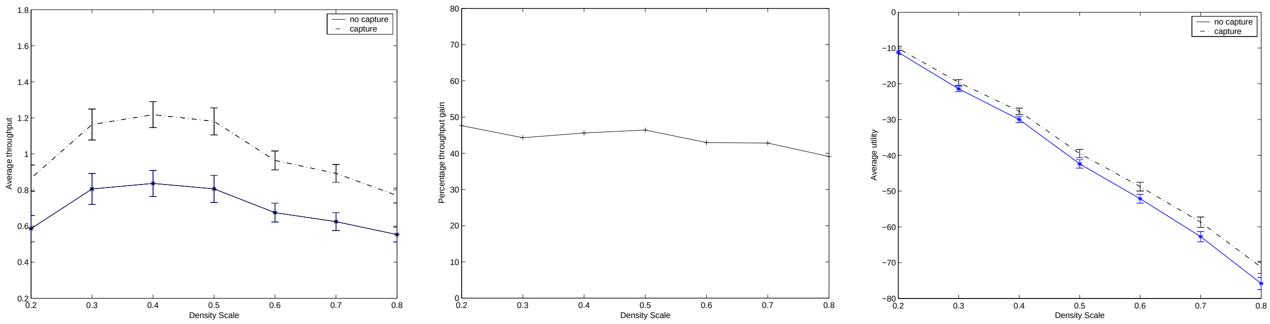

(a) (b) (c)

Figure 6: At $SINR_{th}$= 3.16,(a) Network throughput (b) Percentage throughput gain (c) Network utility at different density scales

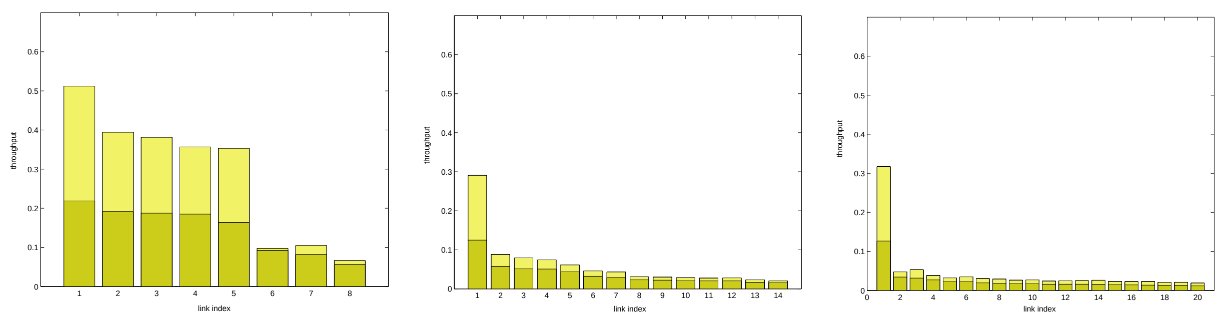

(a)small scale (0.3) (b)medium scale (0.5) (c)large scale (0.8)

Figure 7: Comparing individual session rate at different density scale networks with (light bar) and without (dark bar) capture ($SINR_{th}$ of 1)

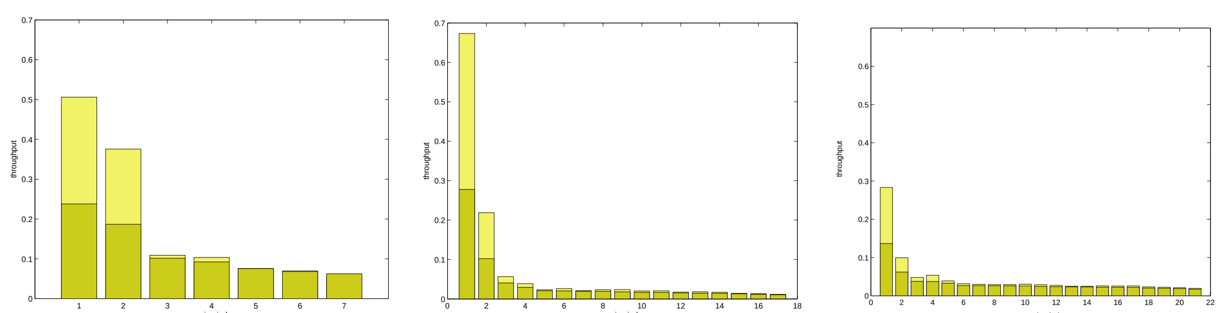

(a)small scale (0.3) (b)medium scale (0.5) (c)large scale (0.8)

Figure 8: Comparing individual session rate at different density scale networks with (light bar) and without (dark bar) capture ($SINR_{th}$ of 3.16)

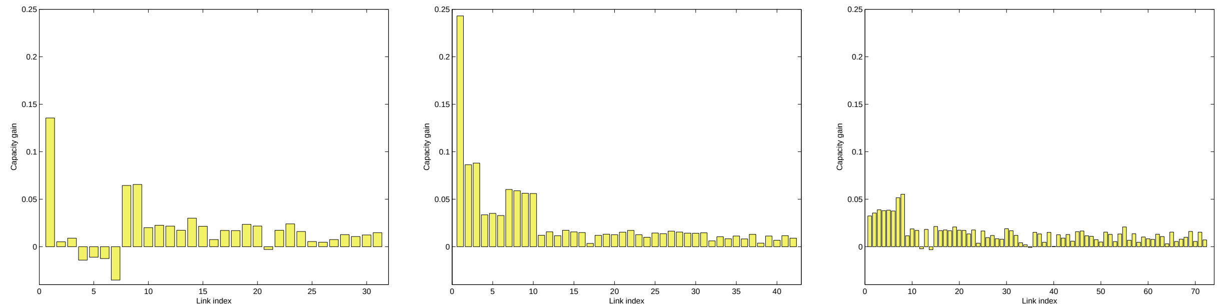

(a)small scale (0.3) (b)medium scale (0.5) (c)large scale (0.8)

Figure 9: Comparing the change in individual link capacities at different density scale network with and without capture ($SINR_{th}$ of 1)

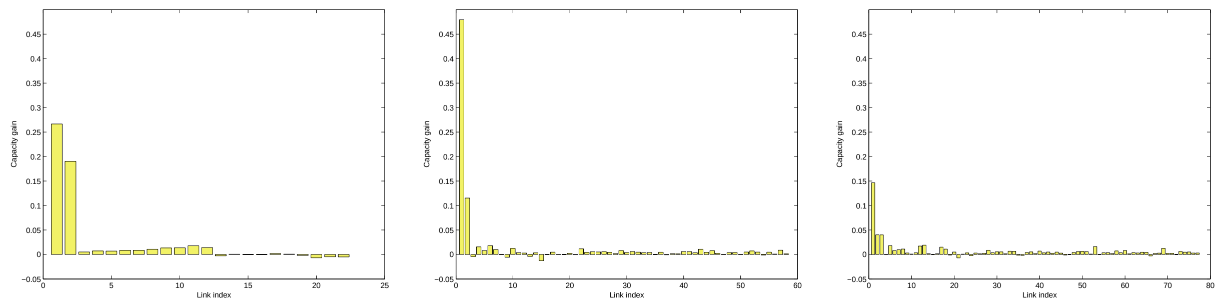

(a)small scale (0.3) (b)medium scale (0.5) (c)large scale (0.8)

Figure 10: Comparing the change in individual link capacities at different density scale network with and without capture ($SINR_{th}$ of 3.16)

8. REFERENCES

[1] Sunil Kandukuri and Stephen Boyd, "Optimal Power Control in Interference Limited Fading Wireless Channels with Outage Probability Specifications", IEEE Journal on Wireless Communications, Volume 1, Number 1, pages 46-55, January 2002.

[2] Xin Wang and Koushik Kar, "Cross-Layer Rate Control for End-to-End Proportional Fairness in Wireless Networks with Random Access", Proceedings of MobiHoc 2005, Urbana-Champaign, May 2005.

[3] http://www-fp.mcs.anl.gov/otc/Guide/

[4] Kamin Whitehouse, Alec Woo, Fred Jiang, Joseph Polastre, David Culler. "Exploiting the Capture Effect for Collision Detection and Recovery." The Second IEEE Workshop on Embedded Networked Sensors (EmNetS-II). Sydney, Australia. May 30-31, 2005.

[5] Dongjin Son, Bhaskar Krishnamachari, John Heidemann, "Experimental Analysis of Concurrent Packet Transmissions in Low-Power Wireless Networks", The 4th ACM Conference on Embedded Networked Sensor Systems (Sensys) , Colorado, USA, Nov 1-3, 2006.

[6] M. Chiang, "To layer or not to layer: balancing transport and physical layers in wireless multihop networks," Proc. IEEE INFOCOM, March 2004.

[7] Lin Xiao, M. Johansson, S.P. Boyd, "Simultaneous routing and resource allocation via dual decomposition", IEEE Transactions on Communications, pp. 1136- 1144, Volume: 52, Issue: 7, July 2004.

[8] Kun Tan, Qian Zhang, Feng Jiang and Xuemin Shen, "Congestion Control in Multi-Hop Wireless Networks", IEEE SECON, September 2005.

[9] N. Abramson, The Aloha System - Another Alternative for Computer Communications, Proceedings of Fall Joint Computer Conference, AFIPS Conference, 1970.

[10] S. Boyd and Lieven Vandenberghe, *Covex Optimization*, Combridge Press, March 2004.

9. APPENDIX

9.1 Derivation of $\alpha_{s,t,k}$ from Outage Probability

The outage probability [1] is

$$\begin{aligned} P(outage) &= Prob(SIR_i \leq SIR^{th}) \\ &= 1 - \prod_{k \neq i} \frac{1}{1 + SIR^{th} G_{ik} P_k / G_{ii} P_i} \end{aligned}$$

Now the probability of success P_{succ} is equal to $1 - Prob(SIR_i \leq SIR^{th})$ which is

$$\prod_{k \neq i} \frac{1}{1 + SIR^{th} G_{ik} P_k / G_{ii} P_i}$$

This equation is in terms of node pair i and $k \in S$ i.e. set of interfering node pairs. In our examples we are taking the path gain G_{ii} for a node pair represented by (i,j) as $1/d_{i,j}^2$, and the transmit power P_i as $TP_{i,j}$. With this notation and simplifying the above equation for the case of just one interfering node k, we get (after a slight rearrangement):

$$\begin{aligned}\frac{1}{1+SIR^{th}G_{ik}P_k/G_{ii}P_i} &= \frac{1}{1+(SINR_{th})\frac{TP_{k,j}/d_{k,j}^2}{TP_{i,j}/d_{i,j}^2}} \\ &= \frac{TP_{i,j}/d_{i,j}^2}{TP_{i,j}/d_{i,j}^2+(SINR_{th})TP_{k,j}/d_{k,j}^2}\end{aligned}$$

9.2 Proof of Convexity Claim

Claim: $\beta_{s,t,k}+\frac{P_k\alpha_{s,t,k}}{1-P_k}$ as well as $\frac{P_k\alpha_{s,t,k}}{1-P_k}-\beta_{s,t,k}$ are both convex.

First it can be shown that $g(P_k)=\frac{P_k\alpha_{st,k}}{1-P_k}$ is a convex function, by double differentiating $g(P_k)$ and verifying that $g''(P_k)\geq 0$. Next, notice that $\beta_{s,t,k}$ is a linear function hence it is convex even when negated. The summation of the convex functions in either case is convex.